Numerical Study of Film Cooling For Various Coolant Inlet Geometries

Prakhar Jindal[#1], A.K. Roy[#2], R.P. Sharma [#3]
[#] Birla Institute of Technology, Mesra, Ranchi, Jharkhand, India
[1] prakharj@bitmesra.ac.in
[2] akroy@bitmesra.ac.in
[3] rpsharma@bitmesra.ac.in

Abstract - The paper deals with the computational investigation of film cooling effectiveness and heat transfer on a 3D flat plate with a cylindrical, elliptic and triangular holes having an inclination of 30^0. Main flow temperature is kept constant at 600K and that of coolant at 300K for all the cases. Centerline and spatially averaged effectiveness are presented for film cooling measurements along non-dimensional temperature profiles in each case. The results for cylindrical case are compared with experimental results and are well in agreement with the experimental results. Comparative studies conducted for the adiabatic film cooling effectiveness and heat transfer coefficient with the three geometries tested (cylindrical, elliptical and triangular hole) reveals that the triangular hole shows much higher effectiveness values than cylindrical case in the near hole region. Also it is observed that triangular hole shows lesser coolant jet height and higher film cooling effectiveness in the region x/D>10, especially at blowing ratios greater than 1.0.

Keywords — CFD, Film cooling effectiveness, Film Cooling.

I. INTRODUCTION

The thermal management and protection of the components and surfaces in rocket engine combustion chambers presents one of the most challenging problems for designers. Film cooling is an active cooling strategy, which involves the continuous injection of a thin layer of protective fluid (coolant) near a wall or boundary to insulate it from rapidly flowing hot propellant gases. Its main advantages are that it allows for the use of much lighter-weight nozzle assemblies and it is relatively simple to implement from a fabrication standpoint. Film cooling is usually measured in dimensionless form known as "film cooling effectiveness", and defined as:

$$\eta = \frac{T_\infty - T_W}{T_\infty - T_C} \tag{1}$$

where, T_w is adiabatic wall temperature, T_∞ is freestream temperature = 600 K, & T_c is coolant inlet temperature =300 K

To study film cooling phenomena, investigators have been using simple geometries to reduce the complexity of the flow affecting the heat exchange between the test surface and the mainstream gas flow. The geometrically simple form of a flat plate with one or more film cooling holes often offers a sufficient approximation of the reality for a lot of research interests. A better understanding of the mechanisms involved in film cooling is needed to achieve an optimized and effective film cooling with a minimum amount of coolant. However, the effectiveness of film cooling is very much dependent on the shape of the injection hole, layout geometry and injection angle.

The aim of the present work is to investigate the effects of the different hole geometry on the flow structure for a 3D flat plate, using k-ε turbulence model.

A. Abbreviations and Acronyms

T_∞	Free stream temperature, K
T_{aw}	Adiabatic wall temperature, K
T_c	Coolant temperature, K
V	Flow velocity, m/s
η	Adiabatic cooling effectiveness
D	Diameter of film hole, mm
l	Length of film hole, mm
M	Mass flux ratio or blowing ratio
ρ_∞	Density of free stream, kg/m^3

ρ_c Density of coolant, kg/m^3

II. LITERATURE REVIEW

Bunker [1] in his comprehensive review paper on film cooling from shaped holes has pointed out that no single shaping of film hole stands as an optimal geometry for all applications. He also concluded that hole shape maintains the cooling jets closer to surface, enhances film coverage and reduces mixing. Also, the shaped holes is used to increase the separation of kidney-vortices which delays the jet lift off and induce a counter-pair of vortices which directly signifies the effect more at high blowing rates.

Goldstein et al. [2-3] reported the effectiveness resulting from a single cylindrical hole and row of holes. They considered a blowing ratio (M) of 0.5 for maximum effectiveness at coolant to freestream DR (Density Ratio) around 1.0. Their results could not justify as found in gas turbine (DR greater than 1.0). Bergeles et al. [4-5] studied the behavior of single discrete jet which was injected normally and at a 30o angle to the crossflow. The authors documented jet lift-off and penetration of the crossflow boundary layer as blowing ratio increased, as well as the influence of the crossflow on the flow within the film hole itself. Andreopoulus and Rodi [6] conducted a detailed analysis of an isolated normal jet in crossflow and found a counter rotating vortex pair downstream of jet injection.

Film cooling effectiveness using a cylindrical hole at an angle of 30, 60, and 90° was studied by Yuen and Martinez [7]. They considered a hole length of L=4D, the free-stream Reynolds number of 8563 based on the free-stream velocity and hole diameter, and the blowing ratio was varied from 0.33-2. For a single 30° hole, in the region immediately downstream of the hole the maximum effectiveness occurred for a blowing ratio less than 0.5. Immediate downstream of this region, centerline effectiveness and lateral spread increased up to a blowing ratio of 0.5, then decreased with increasing blowing ratio due to jet penetration into the free stream. Also, the region with effectiveness greater than 0.2 did not extend beyond x/D=13. Yuen and Martinez [8-9] in their another paper studied the film cooling effectiveness and heat transfer coefficients for a rows of round holes with different hole inclinations.

To study the effect of injecting a small amount of water into the cooling air for film cooling performance, FLUENT was used by T. Wang and X. Li [10]. Their operating conditions were a pressure of 15 atm and a temperature of 1561K. The result showed that 5-10% cooling effectiveness was achieved by 10-20% mist. H.C. Lange et al. [11] investigated the effect of hole imperfection on adiabatic film cooling effectiveness. Film cooling effectiveness was found with the presence of imperfection at different positions. It was founded that the imperfection placed one diameter from the hole leading edge deteriorated the effectiveness at moderate velocity ratios while the same imperfection fixed at the hole exit improved the effectiveness. Influence of different hole shapes on film cooling with CO_2 was investigated by G. Li et al. [12].

III. COMPUTATIONAL METHODOLOGY

GAMBIT 2.4.6 has been used to model the computational domain and also to generate mesh. The governing equations are solved by FLUENT which uses finite volume based solver. In the present study, k– ε turbulence model has been used among several others. In the first part of present study, the results of cylindrical cooling hole have been compared with the experimental study of Yuen et al. [7] as a test case.

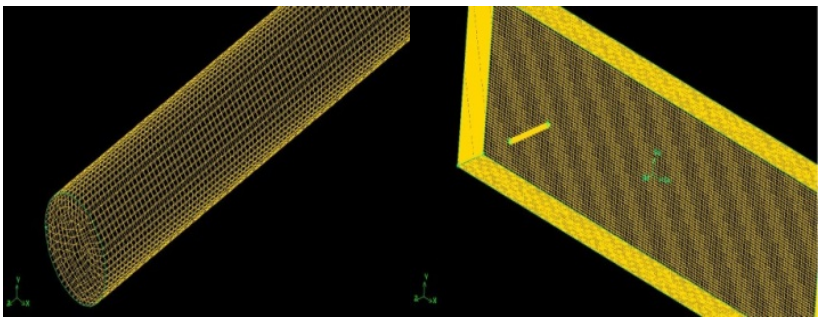

Figure 1: Meshed Geometry for cylindrical hole case

In the literature, they have studied film cooling through single cylindrical hole with streamwise (x-direction) inclination of 30, 60 and 90^o. The geometrical conditions have been kept in coordination with the literature work so as to achieve better comparative results. In the later part of the study, two different shaped holes (elliptic and triangular) have been investigated. The cross-sectional area of other hole configurations used in this work has been kept same as that of cylindrical hole. Fig. 1 shows the meshed geometry of cylindrical hole. For the flat plate surface hexahedral meshes are used while for the cooling hole shapes, hexahedral/wedge

mesh of Cooper type is used.

A. Boundary Conditions:

For the initial study, the geometry consists of a single cylindrical hole inclined at an angle of 300 streamwise having hole diameter 10mm. The L/D ratio is 10. Reynolds number based on freestream velocity and hole diameter is 10364. Blowing ratios ranging from 0.33 - 1.67 have been investigated which corresponds to the coolant inlet velocities (Table 2). Table 1 gives the values of boundary conditions used.

Table 1: Boundary conditions

Conditions	Values
Mainstream Inlet Velocity	15m/s
Mainstream Inlet Temperature	600 K
Density Ratio	1 (approx.)
Coolant Inlet Temperature	300 K

Table 2: Coolant inlet velocities with blowing ratios

S.No.	Blowing Ratio (M)	Coolant Inlet Velocity
1.	0.33	5m/s
2.	0.50	7.5m/s
3.	0.67	10m/s
4.	1.00	15m/s
5.	1.33	20m/s
6.	1.67	25m/s

For grid dependency, the cylindrical hole case for blowing ratio M=0.33 is selected. Different meshes have been tried. Fig. 2 shows the mesh dependency for centerline effectiveness. The different grid size for various meshes is tabulated in the Table 3. From Fig.2 it is clear that the result in case of medium 2 and fine meshes are almost similar but still fine mesh is used for analysis to achieve more accurate results.

Table 3: Different grid size for various meshes

Grid	Cells	Faces	Nodes
Coarse 1	153459	477210	165291
Coarse 2	328161	1012327	347496
Medium 1	634220	1946355	664793
Medium 2	1218504	3722716	1265080
Fine	3818610	11548110	3911869

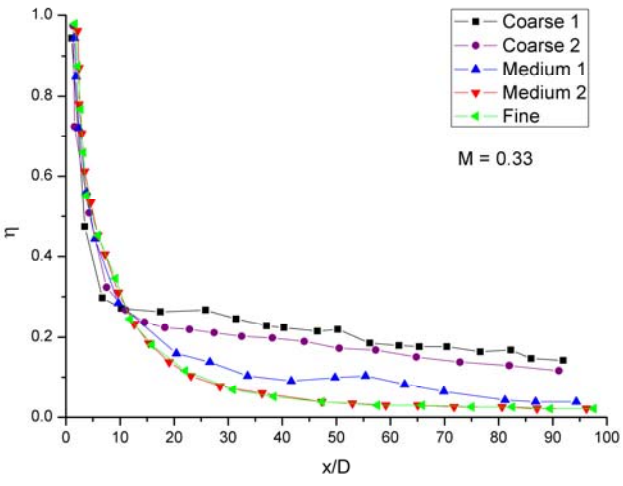

Figure 2 : Grid Dependency Test

B. Solver:

A 3D segregated, steady state solver was used. For linearization of governing equations implicit method was used. For turbulence modeling k-ε model with standard wall functions was used. To avoid use of enhanced wall treatment mesh was kept fine enough to have wall Y+ in the range 0-5.Discretization scheme used was in 2nd order upwind for momentum, turbulence kinetic energy, turbulence dissipation rate and energy, whereas for pressure standard discretization scheme was used. For pressure-velocity coupling SIMPLE algorithm was used. A UDF was used for plotting the centerline effectiveness in all the cases. Convergence is considered to be achieved when the residual values are less than 10^{-4} for continuity equation, 10^{-5} for momentum and 10^{-5} for energy.

C. Governing Equation:

The continuity (2) and momentum (3) equations for the present case of steady state, incompressible, segregated 3D solver and standard k-ε (without viscous heating) turbulence model are:

$$\frac{\partial u_i}{\partial x_i} = 0 \tag{2}$$

$$\frac{\partial}{\partial x_j}(\rho u_i u_j) = -\frac{\partial p}{\partial x_i} + \frac{\partial}{\partial x_j}\left[\mu\left(\frac{\partial u_i}{\partial x_j} + \frac{\partial u_j}{\partial x_i} - \frac{2}{3}\delta_{ij}\frac{\partial u_l}{\partial x_l}\right)\right] + \frac{\partial}{\partial x_j}(-\rho\overline{u'}_i\overline{u'}_j) \tag{3}$$

where,

$$-\rho\overline{u'}_i\overline{u'}_j = \mu_t\left(\frac{\partial u_i}{\partial x_j} + \frac{\partial u_j}{\partial x_i}\right) - \frac{2}{3}\left(\rho\kappa + \mu_t\frac{\partial u_i}{\partial x_j}\right)\delta_{ij} \tag{4}$$

The two additional transport equations (for the turbulence kinetic energy, k, and the turbulence dissipation rate, ε, are solved, and μ_t (turbulent viscosity) is computed as a function of k and ε as:

$$\rho\frac{\partial}{\partial x_j}(ku_i) = \frac{\partial}{\partial x_j}\left[\left(\mu + \frac{\mu_t}{\sigma_k}\right)\frac{\partial k}{\partial x_j}\right] + G_k - \rho\varepsilon \tag{5}$$

$$\rho\frac{\partial}{\partial x_i}(\varepsilon u_i) = \frac{\partial}{\partial x_j}\left[\left(\mu + \frac{\mu_t}{\sigma_k}\right)\frac{\partial \varepsilon}{\partial x_j}\right] + C_{1\varepsilon}\frac{\varepsilon}{\kappa}G_k - C_{2\varepsilon}\rho\frac{\varepsilon^2}{k} \tag{6}$$

$$\mu_t = \rho C_\mu \frac{k}{\varepsilon^2} \tag{7}$$

The model constants known as the turbulent Prandtl number for k is taken as σ_k = 1.0 and the model constant known as turbulent Prandtl number for ε is used as σ_ε=1.3 along with the model constant $C_{1\varepsilon}$, $C_{2\varepsilon}$ and C_μ taken as the default values ($C_{1\varepsilon}$=1.44, $C_{2\varepsilon}$=1.92 and C_μ=0.09) in FLUENT. As these model constant values are standard one and have been found to work fairly well with wide range of wall bounded and free shear flows, hence the same are used for the present computational model.

IV. RESULTS AND DISCUSSION

A. Cylindrical Hole (Single):

The fig. 3 depicts the centerline effectiveness for all blowing ratios (0.33 – 1.67). It is observed that the effectiveness is nearly less or equivalent to 0.2 after *x*/D = 10. In the near hole region effectiveness decreases sharply which may be because of the lift-off of coolant jet due to its momentum. The centerline effectiveness for M 0.33 and 0.5 are very low and can be seen falling below 0.1 after x\D = 25. This may be due to the low momentum of coolant jet as these cases have the lowest coolant inlet velocity among all other blowing ratio cases. Due to increase in the momentum of coolant, an increase in the centerline effectiveness can be seen from 0.33 to 1.67.

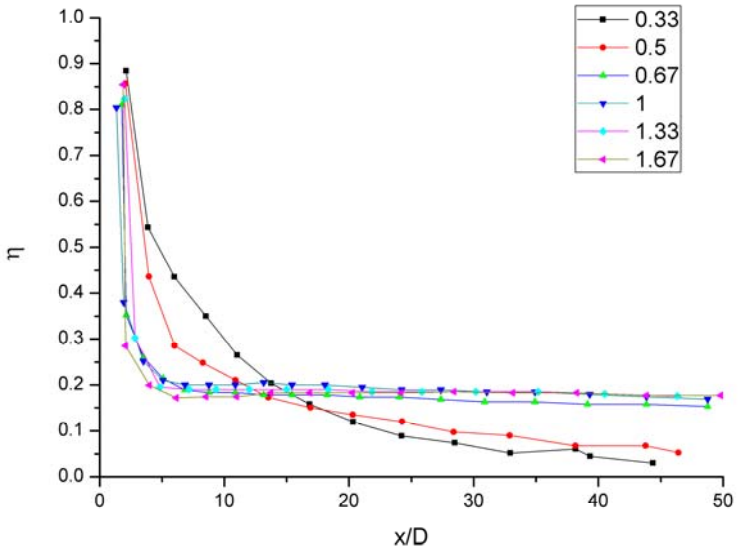

Figure 3: Centerline effectiveness for all M

The performance of different hole shapes for film cooling effectiveness has been measured in terms of centerline and spatially averaged adiabatic film cooling effectiveness. For the validation of CFD results, the case of cylindrical hole is compared with that of experimental data of Yuen et al. [7].

Fig. 4 shows the spatially averaged film cooling effectiveness while fig. 5 shows the centerline film cooling effectiveness for the cylindrical shape. The fig. 4 shows the spatially averaged effectiveness for all the blowing ratios (ranging from 0.33 to 1.67). As it is very clear from the graph that the spatially averaged effectiveness is increasing from blowing ratios 0.33 to 1.0 and then it decreases from blowing ratio 1.0 to 1.67. This shows that the increasing jet momentum is acting a pivot role upto some limit beyond which it contributes towards the jet lift-off and hence decreasing the effectiveness. The value of the effectiveness for all the blowing ratios lies in the range 0.20 to 0.25.

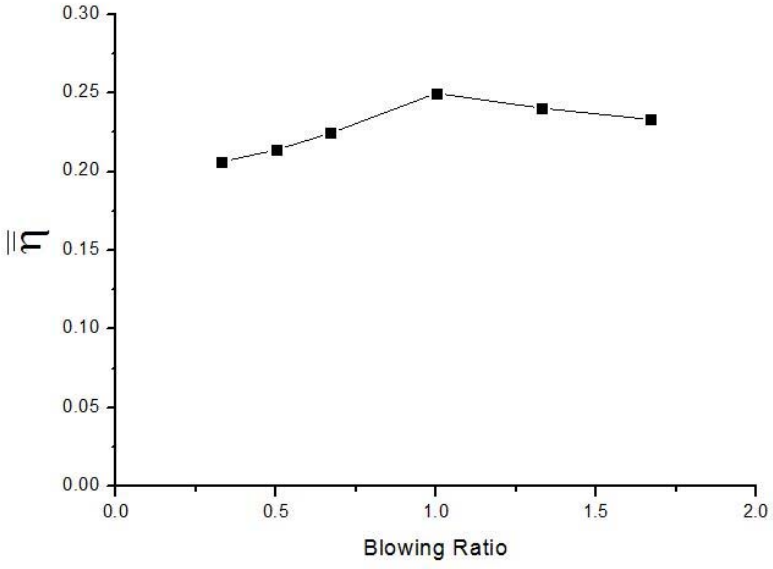

Figure 4: Spatially averaged effectiveness for all M

As can be seen from the fig. 5, the centerline effectiveness is very much in agreement with the experimental results throughout the length except in the near hole region (x/D<5.0). This sudden decrease of effectiveness is might be a result of mainstream penetration into coolant jet or may be due to coolant jet lift-off from the adiabatic surface.

For low blowing ratios (0.33, 0.50), the coolant velocities are smaller as compare to mainstream velocity, the jet liftoff is low as clear from higher centerline effectiveness in the near hole region, the immediate decrease of effectiveness for these low blowing ratios in near hole region is may be due to the penetration of mainstream fluid into the coolant jet while for blowing ratios greater than 0.5, due to the jet lifting-off from the surface the centerline effectiveness decreases to very low values in the near hole region.

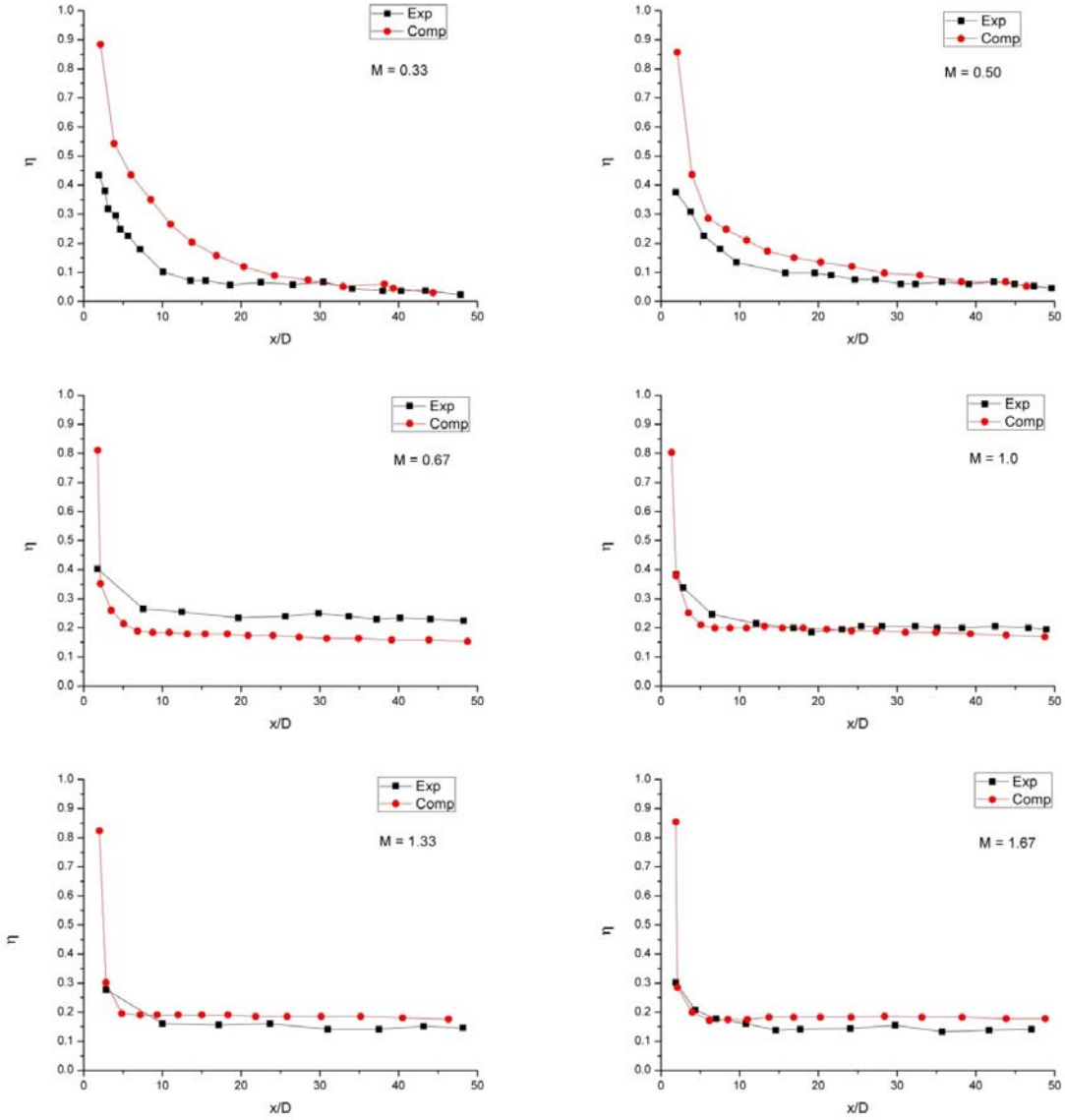

Figure 5: Centerline effectiveness for individual case of blowing ratios (M) for cylindrical hole shapes

The non-dimensional temperature profiles (θ) for all the blowing ratios (0.33 -1.67) has been plotted in fig 6. In the graph, the point θ = 0.0 and 0.1 represents the inlet mainstream temperature (600K) and coolant inlet temperature (300K) respectively. The decreasing values of θ along y/D shows the absence of coolant on the surface. At low blowing ratios (0.33-0.67), resistance to mainstream fluid can be seen due to higher momentum while at high blowing ratios (1.0-1.67) the jet momentum, rather than resisting the mainstream fluid to entrain, is contributing more towards jet lift off.

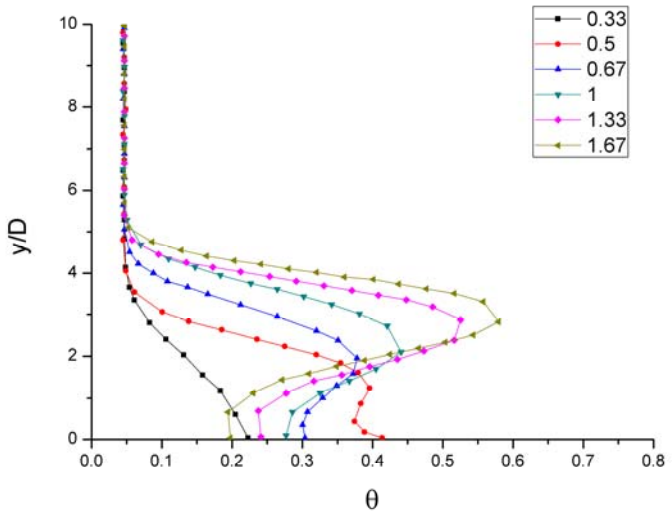

Figure 6: Non-dimensional temperature profile for all M

B. Different Shaped Holes (Single):

The graphs show the effect of different hole shapes on effectiveness. The effect of blowing ratios on different hole shapes (cylindrical, ellipse and triangular) have been shown in figs. 7, 8, 9 respectively. In most of the streamwise region, the effectiveness for all cases decreases with increase in blowing ratios. With the increase of M, the reattachment of coolant jet on the surface is moving forward.

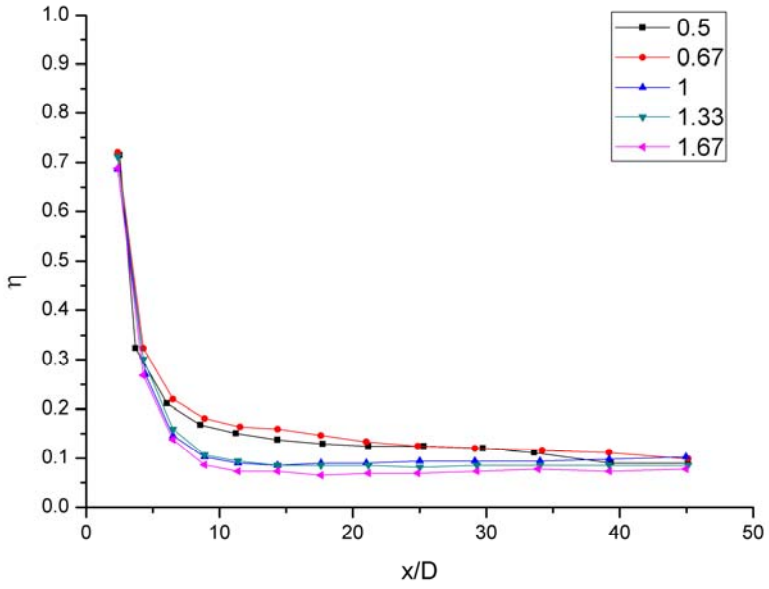

Figure 7: Centerline effective for cylindrical case for all M

This reattachment is prominent in the cylindrical case (fig. 7) at the M=1.0, whereas, reattachment of coolant jet is prominent for M = 1.0 and 1.33 for elliptic case (fig. 8). However, for M = 1.67, very little reattachment is seen after streamwise location of *x*/D ~ 40. The jet reattachment is very prominent at M = 1.0, 1.33 and 1.6 for the triangular case (fig. 9).

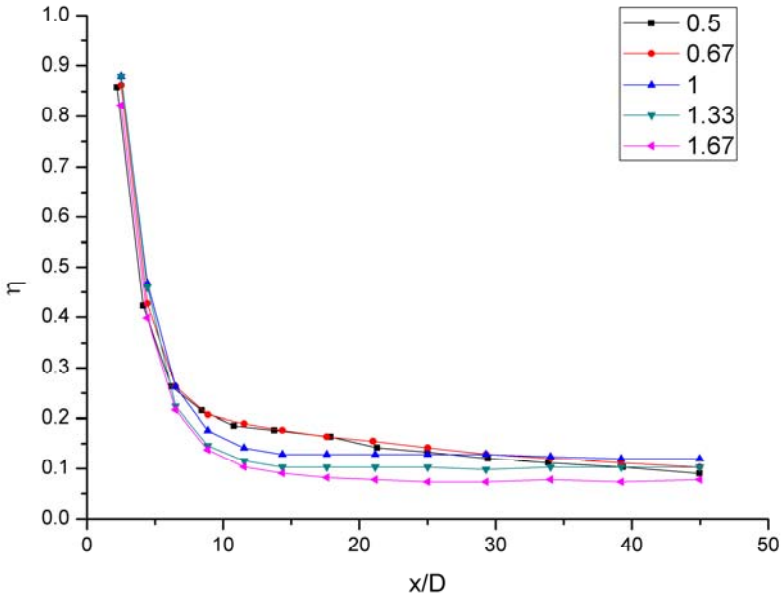

Figure 8: Centerline effectiveness for elliptic case for all M

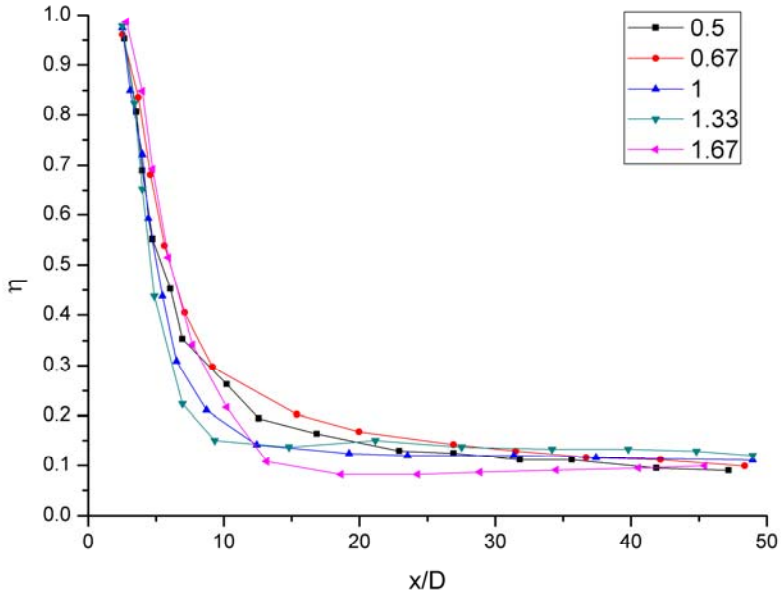

Figure 9: Centerline effectiveness for triangular case for all M

The fig. 10 shows the comparison of centerline film cooling effectiveness for different types of hole geometry (cylindrical, elliptic and triangular) for all blowing ratios. The effectiveness is seen to reduce slowly for all three hole shapes in the case of M = 0.33 along streamwise direction as compared to higher blowing ratios. The jet lift off of coolant jet is less in this case because of low inlet coolant velocity. Among all the hole shape geometries, triangular hole case shows much higher values of effectiveness near hole region upto x/D = 15.

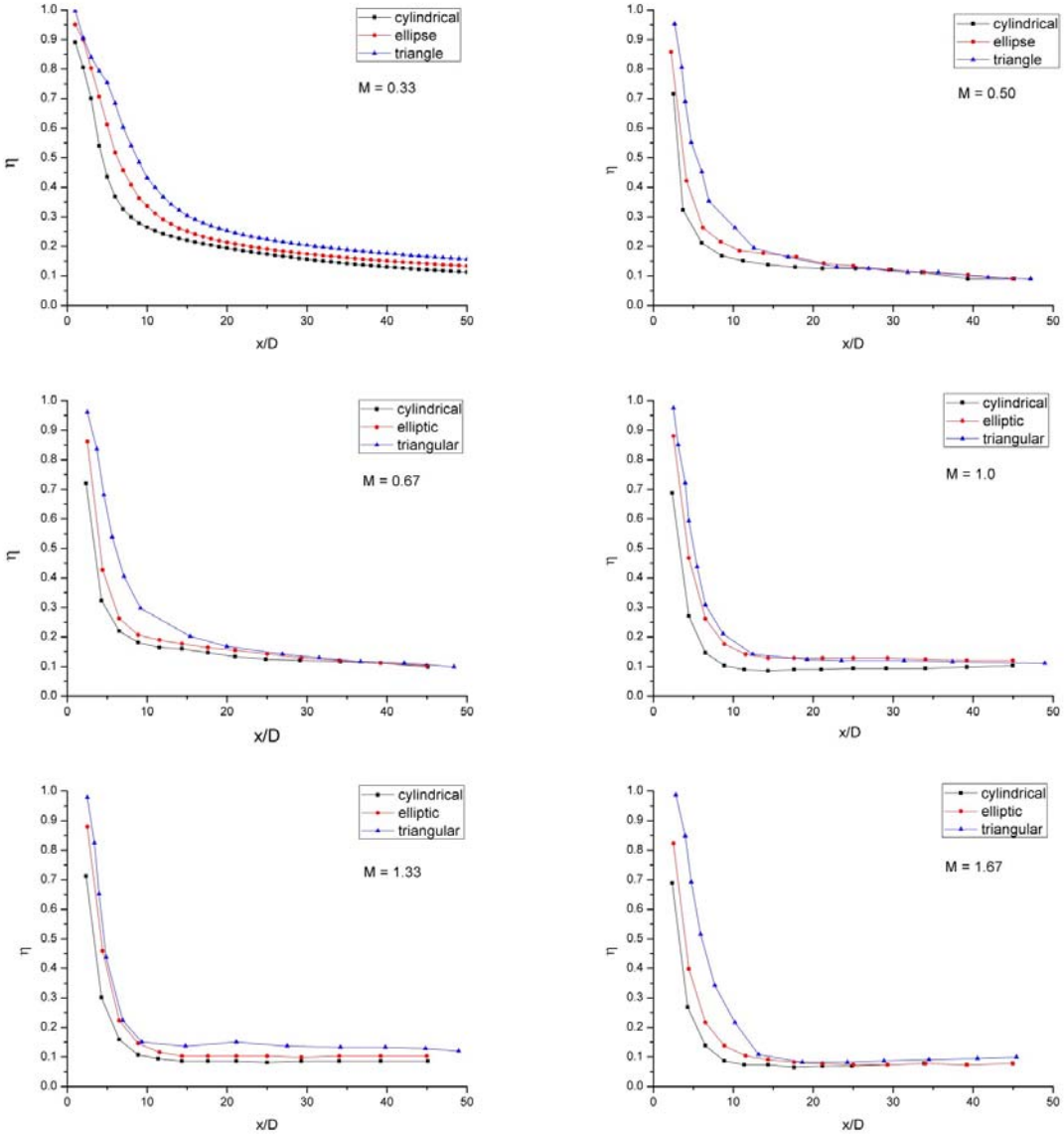

Figure 10: Comparison of Centerline effectiveness case for different hole geometries for all M

After x/D >15, the centerline effectiveness is almost similar to the elliptic values for M = 0.5, 0.67 and 1.0. The centerline effectiveness values for all the blowing ratios remains greater than 0.1 for triangular hole, more than cylindrical and elliptic hole shapes. This may be because of the reattachment of coolant jet with the surface.

The variation of spatially averaged effectiveness with different blowing ratios is shown in fig. 11. In this, the streamwise average is taken over at $1 \leq x/D \leq 10$. A very high lateral distribution of coolant in the region $1 \leq x/D \leq 10$ can be concluded for the triangular hole case as it shows much higher overall effectiveness over the streamwise region.

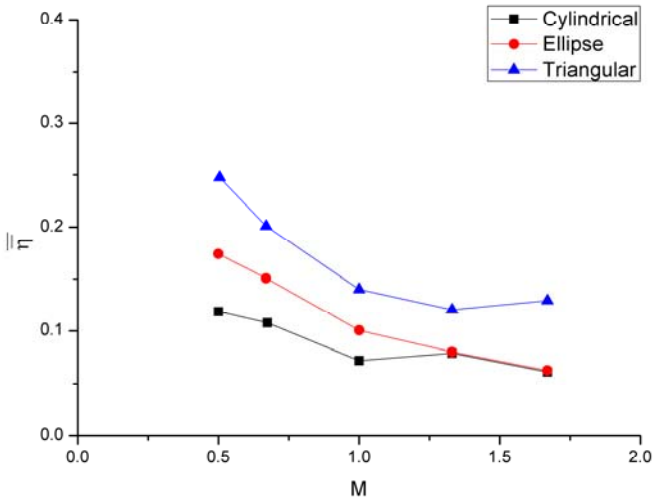

Figure 11: Spatially averaged effectiveness for different hole geometries with M

The centerline non-dimensional temperature (θ) at x/D = 10 for higher blowing ratios (0.67-1.67) has been shown in fig. 12-15. It can be inferred from all the figures that the coolant jet height for all three shapes is almost same for M = 0.67 and 1.0, but for higher M (1.33 to 1.67), the coolant jet height for triangular hole case is much lower than that of cylindrical hole case.

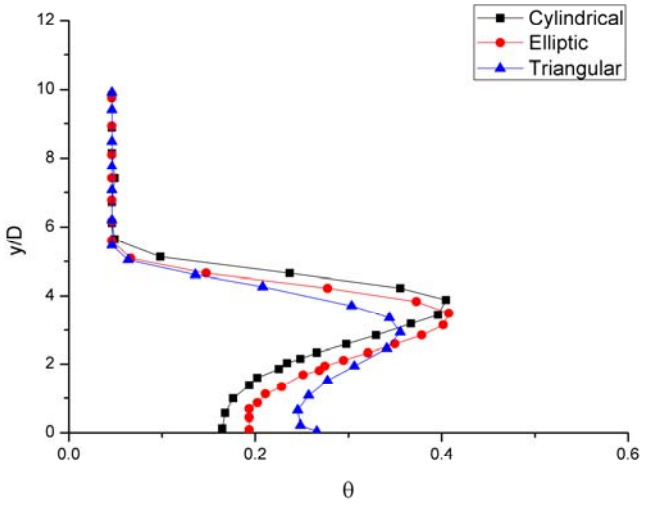

Figure 12: Non-dimensional temperature profile for three hole shapes at M = 0.67

Also the triangular case shows less entrainment of mainstream fluid into the coolant for higher θ values in the lower y/D region near the surface. This results in the higher effectiveness values from the triangular hole case in that region.

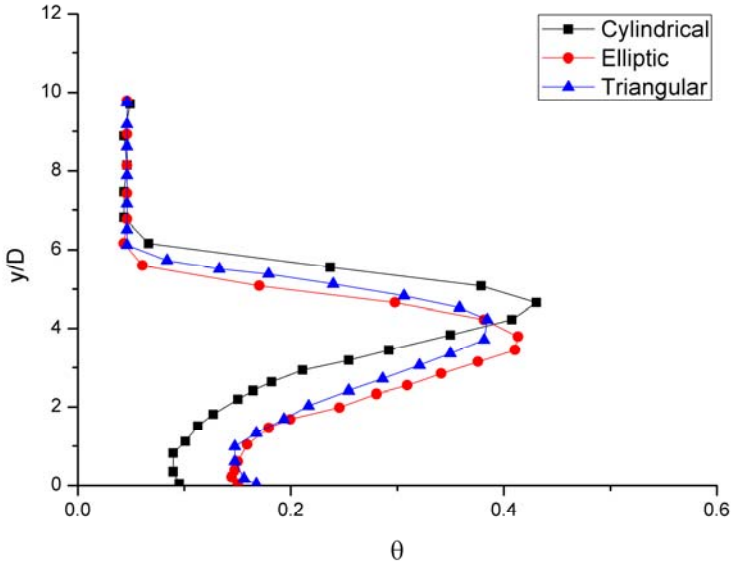

Figure 13: Non-dimensional temperature profile for three hole shapes at M = 1.0

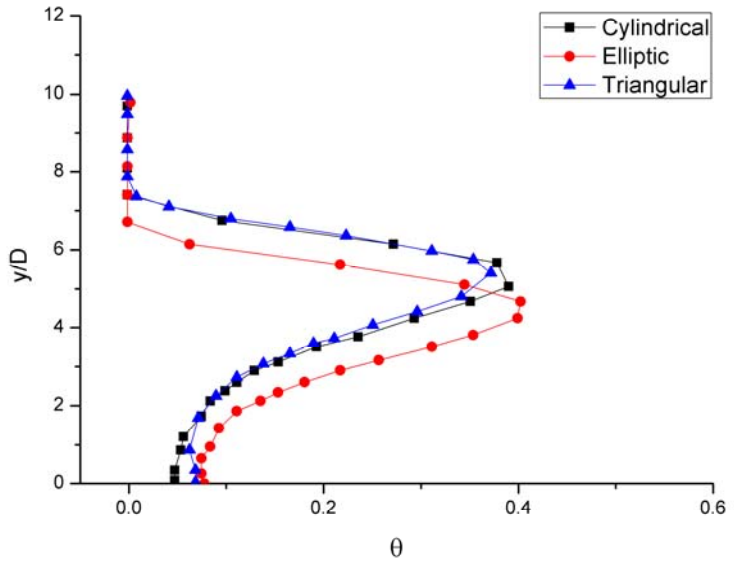

Figure 14: Non-dimensional temperature profile for three hole shapes at M = 1.33

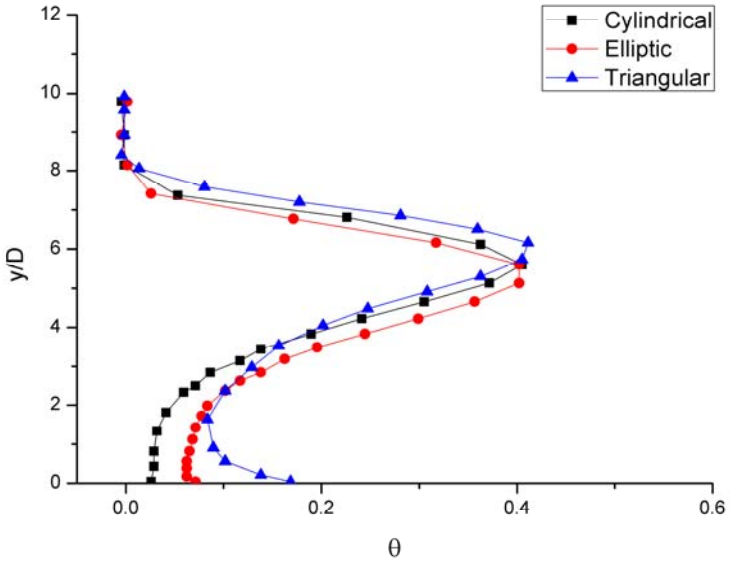

Figure 15: Non-dimensional temperature profile for three hole shapes at M = 1.67

V. CONCLUSION

Various hole shaped geometries have been presented and compared to each other for better results in terms of centerline & spatially averaged film cooling effectiveness. The major conclusions made out of present work are:

1. The experimental work Yuen et al. [7] has been successfully modelled and validated for the computational work.
2. Among the three different coolant hole geometries, triangular hole shape gave the highest centerline film cooling effectiveness in the near hole region.
3. The least jet height was also found out in the case of triangular hole shape which is very less than that of cylindrical hole at higher blowing ratios.
4. The elliptic hole shape show transitional results between other two hole shapes. Hence this hole shape can be considered only for comparison.

REFERENCES

[1] R.S. Bunker, “A review of shaped hole turbine film-cooling technology,” ASME Journal of Heat Transfer, Vol 127, pp. 441-45, 2005.
[2] R.J. Goldstein, E.R.G. Eckert, and J.W. Ramsey, "Film Cooling with Injection through Holes: Adiabatic Wall Temperatures Downstream of a Circular Hole", Journal of Engg for Power, Vol 90, pp. 384-395, 1968.
[3] R.J. Goldstein, "Film Cooling", Academic Press, Chapter-Advances in Heat Transfer, New York, 1971.
[4] G. Bergeles, A.D. Gosman, and B.E. Launder, "The Near Field Character of a Jet Discharged Normal to a Main Stream", Journal of Heat Transfer, Volume 98, No. 3, pp. 373-378, USA, 1976.
[5] G. Bergeles, A.D. Gosman, and B.E. Launder, "Near-Field Character of a Jet Discharged through a Wall at 30 Degrees to a Mainstream", AIAA Journal, Volume 15, No. 4, pp. 499-504, 1977.
[6] J. Andreopoulos, and W. Rodi, "Experimental Investigation of Jets in a Crossflow", Journal of Fluid Mechanics, Volume 138, pp. 92-127, 1984.
[7] C.H.N. Yuen, and Martinez-Botas., "Film Cooling Characteristics of a Single Round Hole at Various Streamwise Angles in a Crossflow: Part I Effectiveness", International Journal of Heat and Mass Transfer, Volume 46, pp. 221-235, 2003.
[8] C.H.N. Yuen, and Martinez-Botas, "Film Cooling Characteristics of Rows of Round Holes at Various Streamwise Angles in a Crossflow: Part I. Effectiveness", International Journal of Heat and Mass Transfer, Volume 48, pp. 4995-5016, 2005.
[9] C.H.N. Yuen, and Martinez-Botas, "Film Cooling Characteristics of Rows of Round Holes at Various Streamwise Angles in a Crossflow: Part II. Heat Transfer Coefficient", International. Journal of Heat and Mass Transfer, Volume 48, pp. 5017-5035, 2005.
[10] T. Wang, and X. Li, "Mist Film Cooling Simulation at Gas Turbine Operating Conditions", International Journal of Heat and Mass Transfer, Volume 51, 5305-5317, 2008.
[11] M.B. Jovanovic, H.C. Lange, and A.A. Van-Steenhoven, "Effect of Hole Imperfection on Adiabatic Film Cooling Effectiveness", International Journal of Heat and Fluid Flow, Volume 29, pp. 377-386, 2008.
[12] G. Li, H. Zhu, and H. Fan, "Influence of Hole Shapes on Film Cooling Characteristics with CO2 Injection", Chinese Journal of Aeronautics, Volume 21, pp. 393-401, 2008.